

Stratigraphic Evolution, Facies Architecture and Reservoir Quality Prediction of Burdigalian Deposits within the “Ekpeti” Oil and Gas Field, Eastern Niger Delta

Joseph Nanaoweikule Eradiri^{1*}, Ayonma Wilfred Mode^{1,2}, Okwudiri Aloysius Anyiam², Ijeoma Maryanna Umeadi¹

¹ Petroleum Technology Development Fund, Department of Geology, University of Nigeria, Nsukka, Nigeria

² Department of Geology, University of Nigeria, Nsukka, Nigeria

Received August 21, 2023; Accepted November 13, 2023

Abstract

A multi-disciplinary approach was employed to study a set of marginal marine sandstone reservoirs within Ekpeti oil field onshore Niger Delta to define discrete facies and their connection with reservoir property trends. Nine wells with accompanying biostratigraphic data were used to build a sequence stratigraphic model while petrophysical and machine learning tools were incorporated to evaluate the reservoirs' potential and establish depositional facies distribution, respectively. This work revealed three fourth-order depositional sequences bounded by erosional surfaces. A total of nine stratal surfaces were delineated which include sequence boundaries (SBs) 13.1 Ma through 21.8 Ma and maximum flooding surfaces (MFSs) 15.9 Ma through 20.7 Ma. The classic three systems tract model (Highstand Systems Tract (HST), Lowstand Systems Tract (LST) and Transgressive Systems Tract (TST)) was adopted in subdividing the depositional sequences into genetically related strata. Incorporating well log facies analysis, results showed the predominant depositional systems within the field general span across the littoral to outer neritic bathymetric zones. A self-organizing map (SOM) algorithm with an added hierarchical clustering technique was used to produce and group nodes that were interpreted as four distinct facies, which correspond to sand, shaly sand, shale and coaly facies. Evaluating the LST and TST marginal marine sandstones revealed very good porosities, low clay volume, high net-to-gross values and significant hydrocarbon accumulations. These results show that depositional facies influence reservoir quality significantly and accurate facies classification can improve the knowledge of the reservoir architecture and help produce more realistic geological models..

Keywords: *Clastic depositional systems; Sandstone reservoir heterogeneity; Petrophysical evaluation; Facies identification; Self-organizing maps.*

1. Introduction

Integrated workflows are vital for understanding subsurface reservoirs and thus reducing uncertainties that encumber the optimal production of hydrocarbons. Geological and geophysical models are continuously designed and updated using new technologies to improve the description of reservoirs. Reservoir quality can be wrongly assessed when the reservoir geology is poorly defined and these errors can have great implications when building three-dimensional (3D) geocellular models and estimating hydrocarbon volumes.

In characterizing oil and gas reservoirs, representing the geological facies accurately is of great importance as it helps to provide a depositional basis for describing the reservoir and understanding the implications for reservoir quality distribution [1-3]. Ideally, core data provides primary information that helps achieve this objective [4-7], however, due to the cost of acquiring core data, accurately defining reservoir and non-reservoir facies within clastic systems still poses a considerable challenge. Because of this, machine-assisted interpretations provide an efficient and cost-effective alternative in facies identification and sorting from geophysical well logs [8].

Spatio-temporal variations in reservoir properties are highly common in clastic, shallow marine deposits, owing to their inherent heterogeneities, primarily due to different rock types and depositional settings [5-6,9-10]. This further necessitates the use of comprehensive methods in unravelling these heterogeneities.

Following the advent of sequence stratigraphy, it has seen widespread use, as it provides a hierarchical approach to studying rock strata and generally reduces uncertainties in field development [11]. This method allows for the recognition of distinct depositional environments and genetic units within a chronostratigraphic framework [12], which in turn informs proper assessment of reservoir potential. Its use in the study of depositional architecture, reservoir continuity and quality distribution is documented in several works [10,13-15]. These studies further confirm that estimating the properties of reservoirs in isolation from their facies distribution, provides only a limited account of the reservoir quality.

Concerning machine-assisted interpretations, several machine-learning tools have been deployed in constraining the interpretation of reservoir geology and properties within siliciclastic and carbonate sequences, including, principal component and cluster analysis [15-16,17], artificial neural networks [18-19], and self-organizing maps [20-21]. Interestingly, in their study [20] discovered that the SOM performs better than other algorithms (artificial neural networks, ascendant hierarchical clustering and multi-resolution graph-based clustering), when correlated with core-derived information, especially with fewer data points.

There are a number of factors that influence reservoir quality variation, including, mineralogical composition, primary depositional facies, diagenetic and structural history, and burial depth [6]. However, before burial, the reservoir quality is primarily influenced by its depositional facies. Therefore, this study focuses on the use of sequence stratigraphic principles and unsupervised machine learning techniques in elucidating the significance of depositional facies on petrophysical properties of clastic reservoirs within the Eketi oil field in the eastern part of the Niger Delta Basin (Fig. 1A).

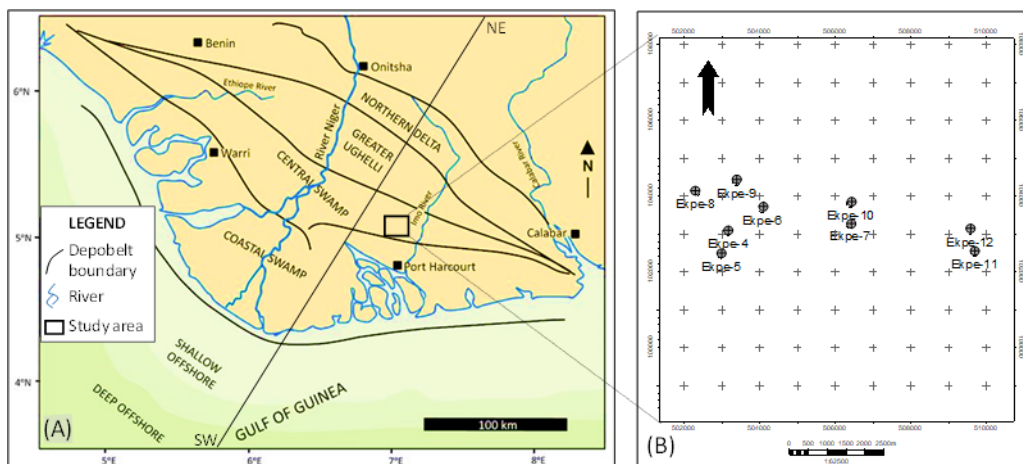


Fig. 1 (A) Simplified map of the Niger Delta, showing the different depobelts and location of the study area. (B) Map of Eketi field showing the location of drilled wells. (modified from [13,22]).

2. Regional geologic setting

The Niger Delta Basin is a generally regressive complex, containing mainly clastic deposits emplaced from the Cretaceous to the Quaternary. The evolution of the Delta is controlled by pre- and syn-sedimentary tectonics [24]. Other factors that controlled the growth of the delta are climatic variations and the proximity and nature of sediment source areas [25]. From the Eocene to the present, the delta has prograded southwestward, forming depobelts that represent the most active portion of the delta at each stage of its development [26] (Fig. 1A). At its core the sediment thickness of the basin is 6km (Fig. 1C) and the total volume is 300,000km² [27]. There are three major lithostratigraphic divisions; the marine shales of the Akata Formation (Palaeocene to Miocene), the fluvio-deltaic deposits of the Agbada Formation

(Eocene to Holocene) and the continental sands of the Benin Formation (Oligocene to Holocene) (Fig 1C). Depobelts divide the delta into distinct structurally defined petroleum systems. Specifically, the field of study is situated in the Central Swamp Depobelt (Fig 1B).

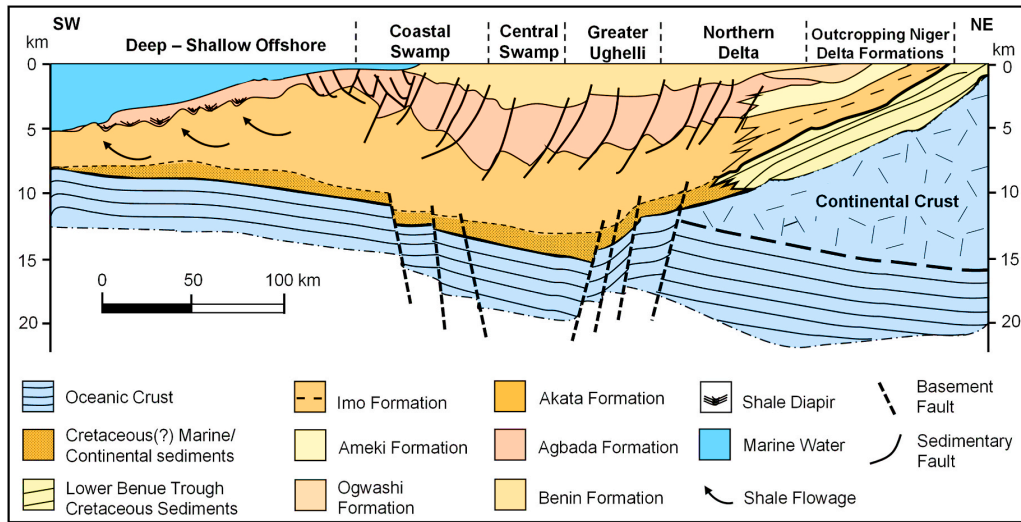


Fig. 1. (C) Schematic of a stratigraphic cross-section of the Niger Delta showing the regional structural setting, depobelts extent and lithostratigraphic units. (modified from [23]).

3. Methodology

The study involved the use of biostratigraphic (including P- and F-Zones) and paleobathymetric data with a suite of conventional well logs from nine wells to produce a sequence stratigraphic framework, interpret the associated depositional facies and characterize key reservoir packages within the field. The biofacies data were calibrated and depth matched with corresponding wireline logs. A sequence stratigraphic framework of the field was built by identifying key surfaces such as sequence boundaries (SBs) and maximum flooding surfaces (MFSs), using a combination of the foraminiferal abundance and diversity plots and motifs from well log curves according to the template [12]. Correlation using marine flooding surfaces within the Niger Delta Basin gives higher confidence, therefore, this method was preferred within the study area. The respective ages of the stratal surfaces were assigned using the Niger Delta zonation scheme [25,28] incorporated with the foraminifera and palynomorph zones (P- and F-Zones) (P740-P670; F9500-F9300) contained in the biofacies data. The three-tract model based on the work of [29] was used in delineating systems tracts [29]. Gamma-ray (GR) log motifs and stacking patterns combined with paleobathymetric data were used to interpret environments of deposition and systems tracts within the field. The Petrel™ software was used for well-log sequence stratigraphic analysis and interpretation.

Additionally, the reservoir properties (shale volume - V_{sh} , porosity - ϕ_{eff} , water saturation - S_w , and net-to-gross - NTG) and the SOM facies analysis of the delineated deposits were done using their respective Interactive Petrophysics (IP™) modules. The V_{sh} was estimated using the [30] equation for Tertiary deposits. The porosity and water saturation module (uninvaded zone) using the modified [31] equation (which is a good general-purpose equation that accounts for the influence of shale) was used to calculate ϕ_{eff} and S_w . The equations used are given below.

$$V_{sh} = 0.083[2^{(3.7*IGR)} - 1.0] \quad \text{---} \quad \text{---} \quad \text{---} \quad \text{---} \quad \text{---} \quad (1)$$

Total porosity (Φ_t) and effective porosity (Φ_{eff}) were estimated using the equations (eqn 2&3)

$$\Phi_t = \frac{\Delta\rho_{mat} - \Delta\rho_{log}}{\Delta\rho_{mat} - \Delta\rho_{fl}} \quad \text{---} \quad \text{---} \quad \text{---} \quad \text{---} \quad \text{---} \quad (2)$$

Effective porosity was estimated for each reservoir interval using the equation below.

$$\Phi_{eff} = \Phi_t - \left\{ V_{sh} * \left(\frac{\Delta\rho_{sh} - \Delta\rho_{mat}}{\Delta\rho_{fl} - \Delta\rho_{mat}} \right) \right\} \quad (3)$$

Water saturation equation based on [31]

$$\frac{1}{R_t} = \frac{\Phi_{eff}^m * S_w^n}{a * R_w} + \frac{V_{sh} * S_w}{R_{sh}} \quad (4)$$

where; Φ_t = total porosity; R_t = true formation resistivity; R_w = resistivity of formation water; R_{sh} = resistivity of shale; n = saturation exponent; m = cementation factor; a = tortuosity factor.

Finally, possible rock types were delineated using the self-organizing map (SOM) algorithm [32] and a hierarchical clustering technique was employed for grouping the SOM clusters to possible geologic facies.

SOM uses a mathematical expression to organize data into groups to produce a map. In this study, the SOM was trained using a spherical geometry with 362 nodes, an initial learning rate of 0.3 and 3000 iterations to give an acceptable distortion value of 0.329. The spherical geometry was chosen in order to reduce the map border effect and decrease inconsistencies associated with the border nodes [33]. Furthermore, the SOM nodes were grouped using hierarchical cluster analysis to produce similar groups which correspond to distinct geologic facies. Gamma-ray and density data from three wells were used as input vectors to train and run the SOM model.

4. Analysis and results

4.1. Lithofacies analysis and depositional environments

Incorporating profiles of gamma-ray logs across and their stacking patterns across all wells [34-35] revealed that the stratigraphic packages within the Ekpeti field were deposited within fluvial/tidal channels, shoreface, shelf and marine environments (Fig. 2). The high energy regime and high volume of sediments within the channels are imprinted as an abrupt (erosional) base and progressively fining upward profile or sharp top as the depositional energy wanes [36] (Fig. 2B). Additionally, the tidally influenced channel sands have a noticeably sharp base and a largely serrated log motif representing intercalations of sand and shale units. However, the profile is generally fining upward, indicating a decrease in energy with time (Fig. 2B). The occurrences of the shoreface deposits within the field showed a distinct funnel profile of a prograding delta and gradual cleaning upward trend [37], (Fig. 2A & B). The upper and lower shoreface are deposited around the shelves and in the outer shelf terrace (below the fair-weather wave base) respectively. The upper shoreface, with lower gamma-ray values, gradually trends into the lower shoreface, with a gamma-ray value of around 60 API, containing sand and shale intercalations (Fig. 2A & B). The delineated shale strata are intervals with > 75 API gamma ray values which contain occasional siltstone units altogether deposited in low-energy environments. Corresponding biofacies information throughout the field showed deposition within coastal deltaic to outer neritic environments. The deepening of the facies is most noticeable towards the eastern portion of the field. The reservoirs of interest were deposited within tidally influenced channels with lesser amounts of shoreface deposits present, they are laterally continuous across all wells and are hydrocarbon-bearing (Fig. 2).

4.2. Sequence stratigraphy

All wells within the field contained biostratigraphic data and were correlated to build a sequence stratigraphic framework. Ekpe-5 served as a control well for the analysis, seeing that it penetrated all the depositional sequences. This study revealed four 3rd-order depositional sequences defined using associated sequence boundaries (SBs) based on the [29] scheme. The depositional sequences are characterized by three MFSs and SBs dated 20.7 Ma to 15.9 Ma and 21.8 Ma to 13.1 Ma respectively (Fig. 3). The foraminiferal and palynological zones used to assign the ages of the sediments are P720 to P630 and F9500 to F9300, respectively, which showed the sediments are Aquitanian to Serravallian in age (Fig. 3). Three major systems

tracts (highstand, transgressive and lowstand) were found in all the four sequences. The following discussion details paleoenvironmental implications resulting from the interplay between eustacy, sedimentation rate and accommodation space for each depositional sequence.

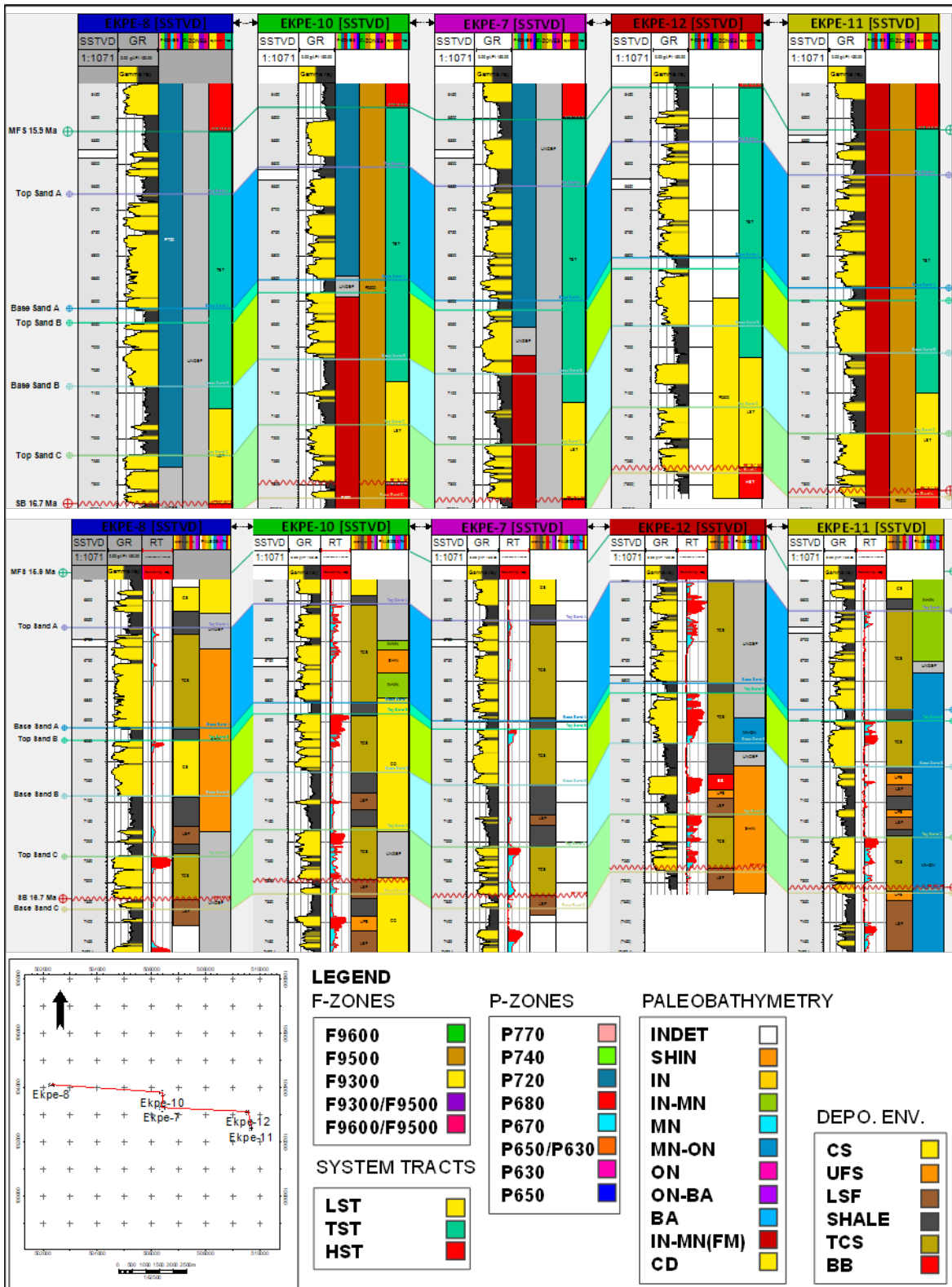


Fig. 2. Lithofacies interpretation within the delineated reservoir interval in the field.

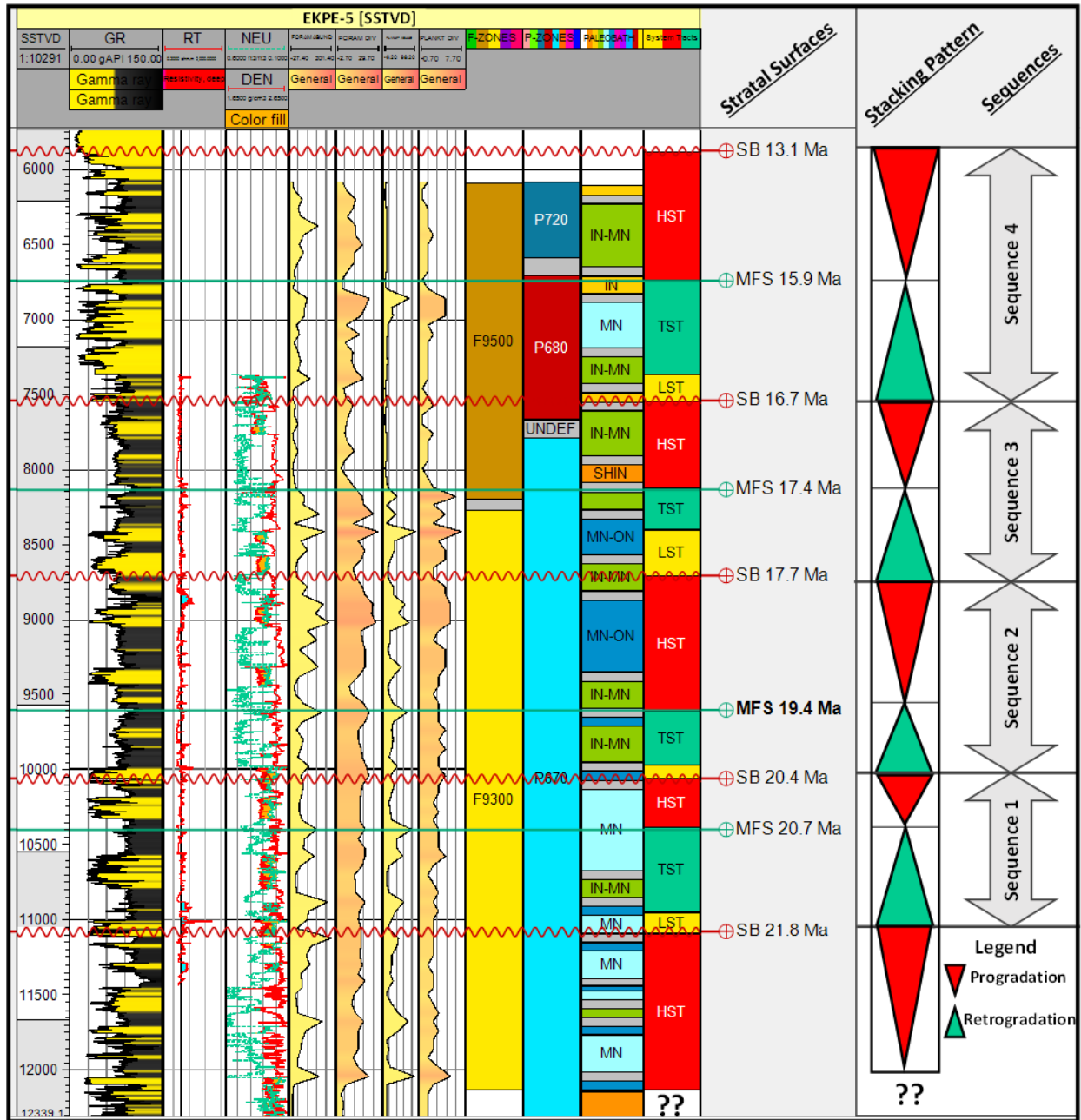


Fig. 3. Sequence stratigraphic tools from a type well within the field.

4.2.1. Depositional sequence 1

This sequence was penetrated completely by well Ekpe-5 and partially by Ekpe-11. Bounded at the top by SB-21.8 Ma and base by SB-20.4 Ma, it had a 1.4 Myr depositional duration. Following the influx of continental sands into the depocenter, channel sands were deposited forming an LST, which was then preceded by a shale unit that signifies the onset of marine transgression. The channel sand is relatively thin, which could imply a lower sediment supply that was outpaced by the rate of creation of accommodation space as time passed (Fig. 4). During this episode of extended marine incursion, transgressive to regressive shoreface sediments were deposited within the TST, with the sea reaching a maximum flooding level around 20.7 Ma. Progradation of the facies resumed within the HST, resulting in an expected increase in the sand-to-shale ratio when compared with the TST. The sediments within the HST are

mainly delta front/shoreface sands and shelf mudstones and the entire sequence is about 1000 ft thick (Fig. 4).

4.2.2. Depositional sequence 2

Three wells penetrated this depositional sequence (Fig. 4). It is bounded at the base by SB-20.4 Ma and capped at the top by SB-17.7 Ma, indicating that the depositional cycle was completed in 2.7 Myr. The LST deposits that begin the sequence contain channel sands capped by a shale layer which was the first occurrence of more distal facies. As accommodation space was created, and base level increased it was not met with sufficient sediment influx, causing the TST to be mud rich, with minor amounts of heteroliths and sandstones that appear to be deposited within a lower shoreface environment (Fig. 4). The top of the TST is defined by the 19.4 Ma MFS, which is followed by a noticeable fore-stepping of the facies as sediment flux increased within the HST. The highstand systems tract is characterized by shoreface sandstones and shales, possibly deposited in the lower fringes of the shelf. The total thickness of the sequence is about 1,100 ft.

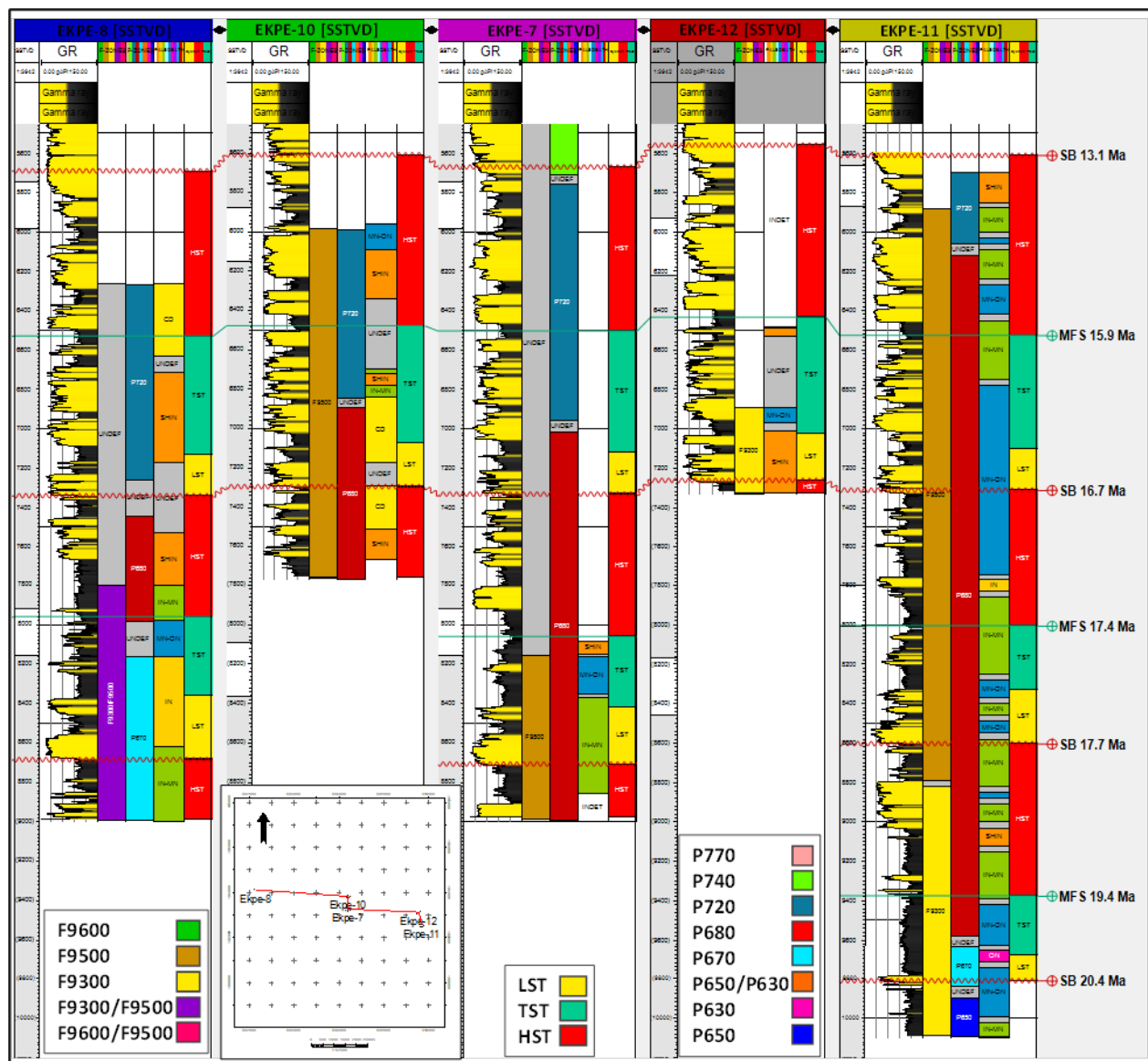


Fig. 4. Strike-wise sequence stratigraphic correlation (inset: base map of wells used, legend for F-Zones, P-Zones and systems tracts).

The farthest extent of the sea level was reached at an age of 17.4 Ma, where there is a noticeable deposition of a black marine shale interpreted from considerably higher gamma-ray values (255 – 131 API) (Fig. 4 and 5). As the sea level began to decline, the HST sands and shales were deposited, with roughly aggradational parasequence sets in the vicinity of well Ekpe-5 downdip, and a progradational stacking pattern in the up-dip wells (Fig. 5). Sand-to-shale ratio generally increases through time and the entire sequence is about 1,380 ft thick.

4.2.4. Depositional sequence 4

This is the youngest depositional sequence in the field and it is defined by SBs 16.7 Ma and 13.1 Ma, respectively. The depositional cycle lasted for 3.6 Myr, beginning with the deposition of a channel sand within the LST when the sea level was at its lowest. This sand overlies the shoreface sediments of the underlying HST. As the sea level increased, there was creation of accommodation space accompanied by a high influx of sediments, prompting the deposition of a set of tidally influenced channel sands with individual fining upward profiles and an overall aggradational succession (Fig. 5). These represent the main deposits within the TST. The faunal marker *Chiloguembelina 3* was used to characterize the 15.9 Ma stratal surface at a depth of 6527 ft. in well Ekpe-11 (Fig. 4), which marked the beginning of the fall in sea level. The HST in this sequence is thicker, with a higher sand-to-shale ratio than in the older sequences, which implies much more influx of continental sands with time and minor marine input. The highstand paleoenvironments of deposition are mainly distributary channels and delta front with minor shelf deposits. The total thickness of the sequence is approximately 1,676ft (Fig. 5).

4.3. Reservoir quality assessment

Three reservoirs were evaluated within the field (Reservoirs A, B and C), all of which are within depositional sequence 4 (with the highest sand development); the results from their petrophysical analysis are detailed and interpreted below. The porosity values were described using thresholds based on [38].

4.3.1. Petrophysical evaluation

The youngest reservoir within the sequence, reservoir A, has an average total thickness of 245.3 ft. while on average, the net sand thickness is 193.25 ft. (79%). Sand development decreases towards the eastern part of the Ekpeti field (Ekpe-10 to Ekpe-12; about 3km). The reservoir possesses a very good average porosity of 0.29 v/v and a volume of clay value of 0.05 v/v. The negligible clay volumes show that the reservoir properties are not greatly affected by the fines distributed within. There is a decent amount (27%) of hydrocarbon accumulated within this reservoir. Reservoir A is a stack of tidally influenced channel sandstones.

Table 1. Results of petrophysical analysis of Reservoir A across the three wells.

Well Name	Top (ft.)	Bottom (ft.)	Gross (ft.)	Net (ft.)	N/G (%)	Av. Phi (v/v)	Av. S _w (v/v)	Av. V _{clay} (v/v)
Ekpe-10	6614	6854	240	192	0.80	0.29	0.83	0.06
Ekpe-7	6655.5	6907	251.5	207.25	0.83	0.24	0.95	0.04
Ekpe-12	6552.5	6797.5	244.5	180.5	0.74	0.35	0.42	0.04
AVG	-	-	245.33	193.25	0.79	0.29	0.73	0.05

Reservoir B possesses a very high sand-to-shale ratio of 91%, with a gross thickness of 135.5 ft. and a net sand thickness of 123.08 ft. Net sand decreases across the field. Given the high values of sand-to-shale ratio, porosity values are very good with the evaluation showing an average of 0.29 v/v. The clay distribution within this reservoir is negligible with an average value of 0.04 v/v throughout the reservoir. Hydrocarbon saturation is relatively higher in reservoir B with a concentration of 40%, this points to a favourable quantity of exploitable hydrocarbons. The hydrocarbon saturation is highest in the vicinity of Ekpe-12 which showed a value of 80 v/v.

Table 2. Results of petrophysical analysis of Reservoir B across the three wells.

Well Name	Top (ft.)	Bottom (ft.)	Gross (ft.)	Net (ft.)	N/G (%)	Av. Phi (v/v)	Av. S _w (v/v)	Av. V _{clay} (v/v)
Ekpe-10	6885.5	7027	141.5	128.75	0.91	0.28	0.75	0.05
Ekpe-7	6934.5	7076	141.5	130.25	0.92	0.24	0.86	0.02
Ekpe-12	6829.5	6953	123.5	110.25	0.89	0.34	0.20	0.05
AVG	-	-	135.50	123.08	0.91	0.29	0.60	0.04

Reservoir C, the oldest reservoir within the evaluated interval possesses an average net-sand value of 74%, with 141.83 ft. and 104.5ft. of gross- and net-sand thicknesses, respectively. Comparatively, the reservoir has finer sediments than reservoirs A and B, and therefore, the lowest net-to-gross value. The average porosity is very good, with a value of 0.29 v/v and minor amounts of volume of clay estimated to be 0.05 v/v. Hydrocarbon saturation across all the wells is highest here, with an average value of 54%. Reservoirs B and C are made up of tidal channel sands deposited upon upper shoreface sandstones. The tidal sands, however, make up the bulk of the sand volume within these reservoirs.

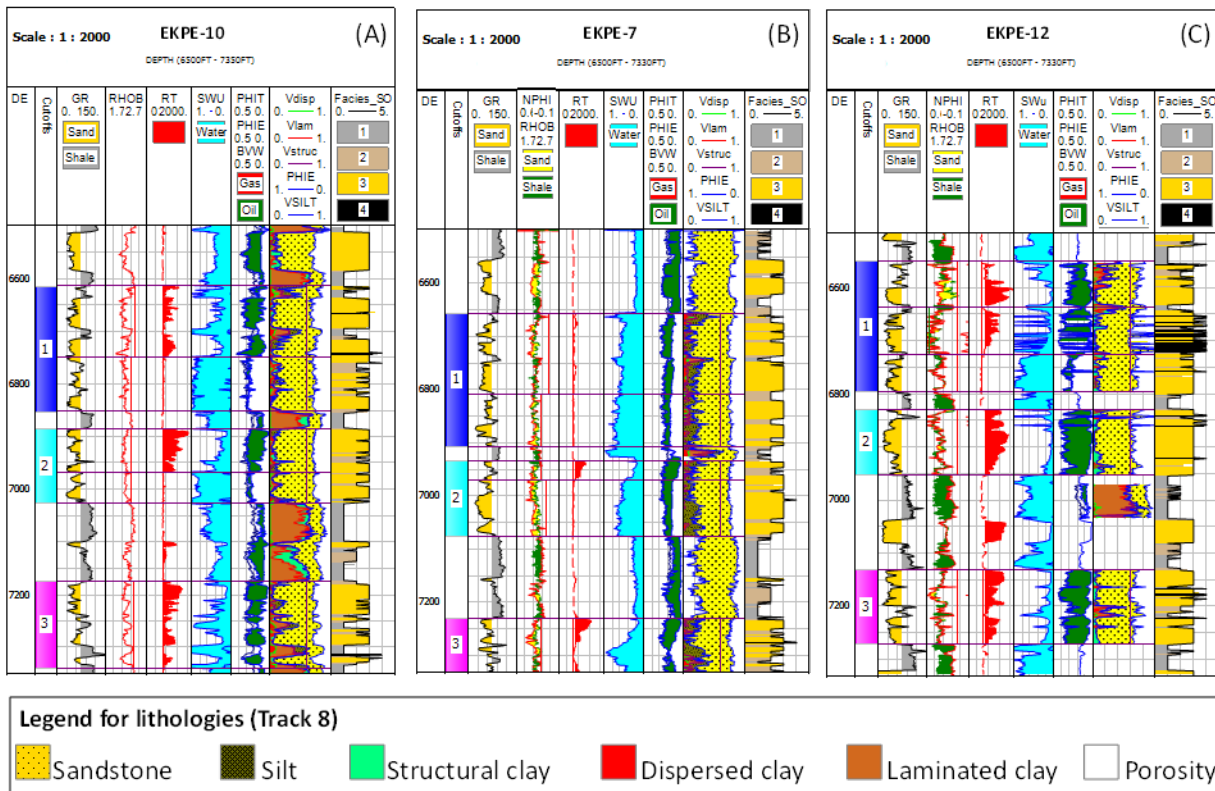


Fig. 6. Well log petrophysical assessment showing results from the evaluation and delineated SOM facies.

Table 3. Results of petrophysical analysis of Reservoir C across the three wells.

Well Name	Top (ft.)	Bottom (ft.)	Gross (ft.)	Net (ft.)	N/G (%)	Av. Phi (v/v)	Av. S _w (v/v)	Av. V _{clay} (v/v)
Ekpe-10	7174	7300	166	112.5	0.68	0.28	0.50	0.07
Ekpe-7	7231	7351.5	120.5	86.25	0.72	0.24	0.62	0.02
Ekpe-12	7132.5	7271.5	139	114.75	0.83	0.34	0.25	0.05
AVG	-	-	141.83	104.50	0.74	0.29	0.46	0.05

All three reservoirs are sand-rich with very good porosities and high net-to-gross values. The hydrocarbon saturation is high and volume of clay within the reservoirs is negligible and

does not overly exert any influence on other petrophysical values (Fig. 6; Table 1, 2 and 3). Critical observation at some intervals within the reservoirs, especially in the vicinity of well Ekpe-12 shows noticeably high porosity (35% to 41%), which is attributed to the rather low density and high neutron values at those intervals.

4.3.2. SOM petrofacies distribution

Following the SOM model build and run, four SOM facies were revealed from the analysis. The randomness of the data was examined to derive the appropriate number of groups to be used in the clustering method, with four being the ideal number (after which adding more clusters will result in more randomness and hence more noise) (Fig. 7A).

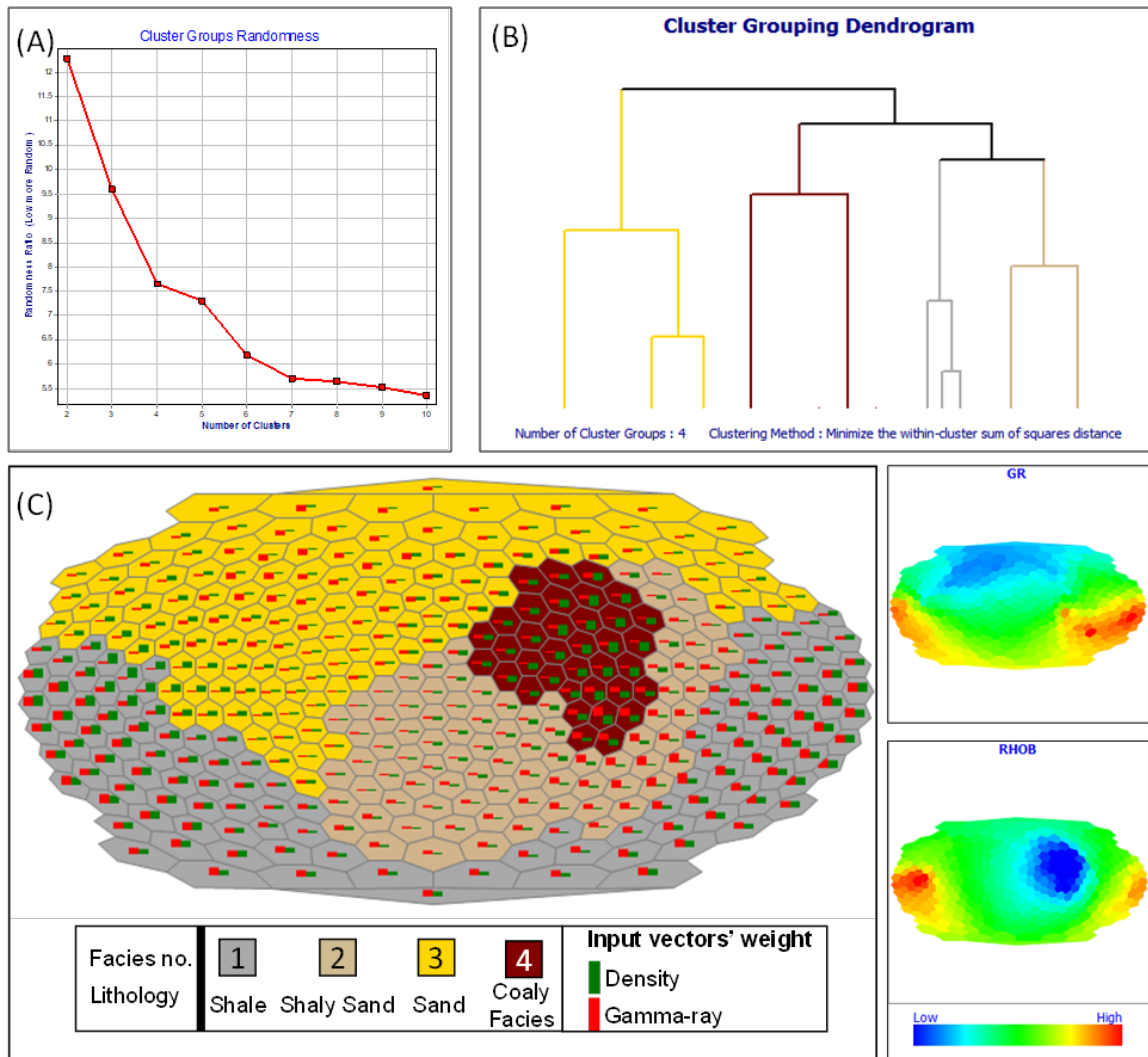


Fig. 7. SOM facies delineation. (A) Cluster randomness plot. (B) Dendrogram generated for grouping SOM clusters. (C) SOM facies grouped to corresponding nodes, with the weight of input vectors shown as bars.

Subsequently, nodes within the SOM with similar vector weight, were grouped using a hierarchical clustering technique as seen in the dendrogram (Fig. 8A), which produced four distinct groups interpreted geologically as clean sand, shaly sand, shale and coaly facies (Fig. 8C). The sand intervals have low gamma-ray and moderate density values (<60 API and 1.9-2.2 g/cm³), the shaly sand units both typically showed moderate gamma-ray and density values (60-85 API and 2.0-2.3 g/cm³). The typical non-reservoir units, shale and coaly facies, displayed high gamma-ray and high-density values (>80 API and >2.2 g/cm³), and, low-moderate gamma-ray and very low-density values (<50 API and <1.8 g/cm³), respectively.

The distribution of each petrofacies is not uniform within correlatable reservoir units; however, this is most notably peculiar with the coaly facies which are predominant towards the eastern part of the field (in well Ekpe-12) (Fig. 6C). While the gamma-ray log shows only two main lithologies (based on natural radiation emitted), the density log as an additional input vector in the SOM helped detect a third and fourth facies (shaly sand and coaly facies). The coaly facies delineation is further constrained by superposing the density and neutron porosity logs, which show a deflection of both curves towards the left part of the track in well Ekpe-12, indicating low-density values and high levels of hydrogen nuclei concentration (Fig. 6C).

5. Discussion

5.1. Stratigraphic evolution and depositional environments

The field's stratigraphy is predominantly characterized by an assortment of clastic deposits in varying depositional environments within different bathymetric zones. As eustacy, sediment supply and accommodation space changed through the Early to Middle Miocene, these factors influenced the depositional styles and thus facies architecture of the packages within the field. There is a noticeable overall progradation of the facies, which is apparent from the increase in the ratio of sand to shale through geologic time (Fig. 4). The shoaling-upward profile shows an increasingly dominant fluvial supply responsible for the building out of the Delta. Two distinct episodes of high sediment influx coupled with low accommodation space produced thick sand packages associated with sea-level falls at 17.7 and 16.7 Ma which were likely incised valley fills [10,25]. Tidal and wave influence on sedimentation styles is also apparent across the field, it is established by the occurrence of tidally influenced sandstones and shoreface deposits which formed as delta front sediments were reworked by longshore drift currents (Fig. 8). These processes caused the reservoirs to be mainly found as fluvial and tidal channel sands, and shoreface packages, an observation which is common within the Agbada Formation of the Niger Delta and supports the works of [39-41]. Based on bathymetric profiles, the shales within the study area are open marine, shelf and floodplain fines, while the coals were deposited within a swamp in a delta plain setting during a period of marine transgression (Fig. 8). Sand and coaly sequences (Fig. 8) are most likely due to lobe switching of the river channel and deposition of interdistributary bay coaly facies. The presence of coaly facies in the Early Miocene deposits has also been reported in the works of [6,25].

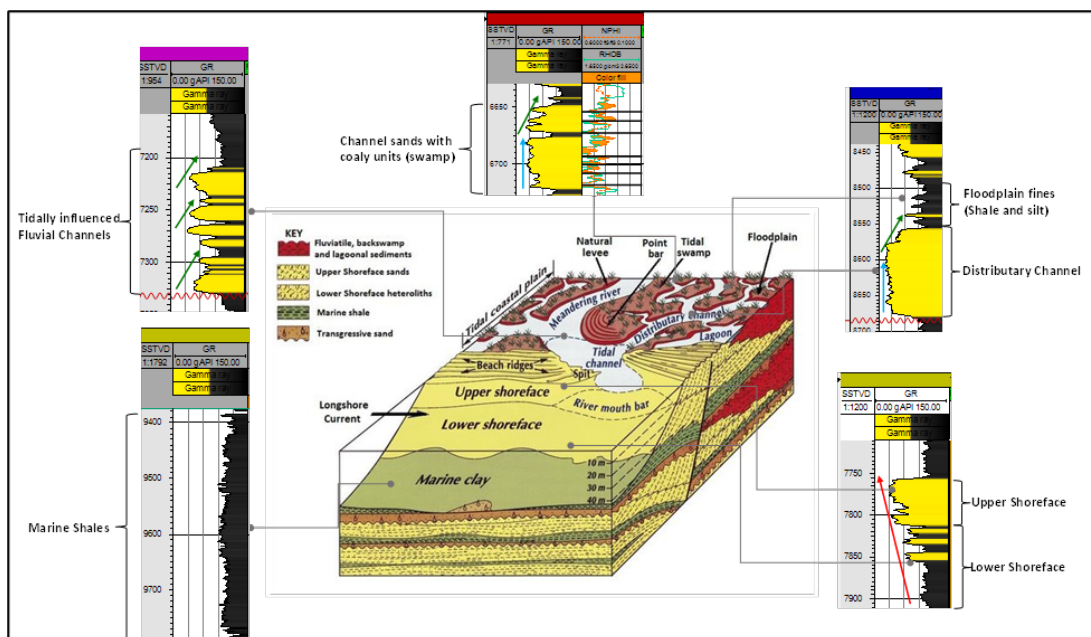


Fig. 8. Conceptual depositional model of a coastal zone of the Niger Delta Basin with corresponding GR log responses showing different geomorphological features, environments and facies modified after [42].

Regarding the delineated reservoirs, they were deposited during a lowstand (Reservoir C) and in a subsequent rise (Reservoirs A & B), accompanied by a relatively higher (compared to previous transgressive cycles) sediment flux into the basin. This gave rise to shoreface sands capped by fluvial channel deposits influenced occasionally by tides.

5.2. Facies architecture and reservoir behaviour

All the studied reservoirs are sand-rich; however, minor associated shale units and coaly facies are also present in them, making up non-reservoir facies. Generally, coastal deltaic and shallow inner-neritic sandstones tend to have good reservoir quality [6,10]. However, the heterogeneities of these sandstones can hamper producibility [36]. The proportion of reservoir to non-reservoir facies is high within the delineated packages, with sand and shaly sand composition at about 86%, 96% and 85% for reservoirs A, B and C, respectively (Fig. 9).

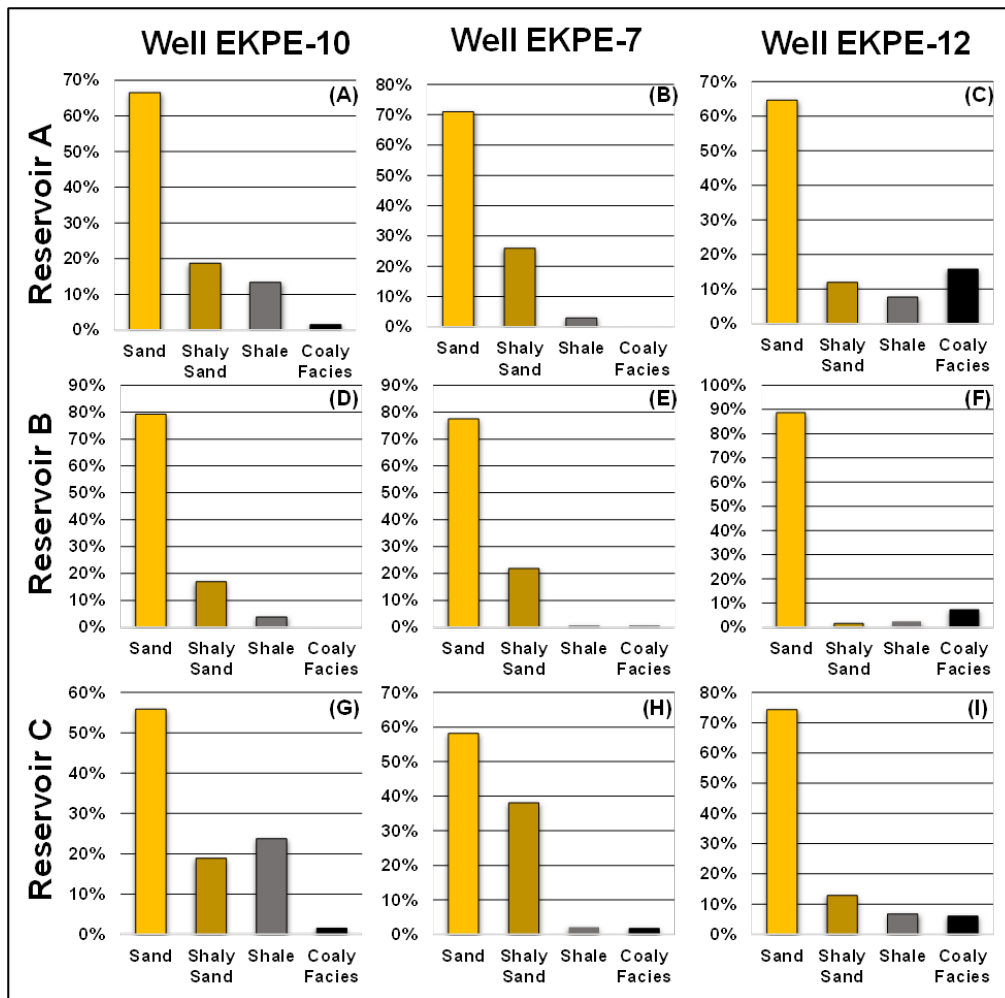


Fig. 9. Percentage distribution of the four delineated SOM facies within the evaluated reservoirs across the three wells.

Given their rich sand development, the quality of these reservoirs is generally good and they all possess excellent net-to-gross. Additionally, their facies distribution shows that non-reservoir units (shale and coaly facies) are in minor amounts (Fig. 9). Reservoir quality as evaluated from the sandstone petrophysical analysis, shows that these non-reservoir facies only have a minor consequence on petrophysical parameters. The associated clays are mainly structural and laminar in form and have only a minimal effect on the reservoir quality. However, without the help of such tools as the SOM, the quantity of facies such as coaly facies can

be wrongly delineated as sandstones, thereby affecting key petrophysical values that ultimately serve as inputs in hydrocarbon volume estimation. Furthermore, when these reservoirs' flow characteristics are examined, the presence of such intra-reservoir shales within shoreface and tidally influenced reservoirs, for example, could adversely affect vertical and lateral permeability [43]. The coaly units within the delta plain portion of the reservoirs could also serve as possible barriers to fluid flow which tend to impact the efficiency of enhanced oil recovery operations [37].

6. Conclusion

Nine major strata-bounding surfaces (including five SBs and four MFSs) were delineated and used to build a chronostratigraphic framework of four third-order depositional sequences. A mixed fluvial, tidal and wave influence on the overall prograding delta in the Early to Middle Miocene is also apparent.

Gamma-ray log facies analysis integrated with biofacies data reveals that the field is characterized predominantly by fluvio-deltaic sequences, including; fluvial and tidal channels, coastal plain and swamp facies, and shoreface deposits. Considerable facies change occurs downdip and eastwardly in the study area as the sand-to-shale ratio decreases.

The three delineated reservoirs were deposited during an episode of sea-level rise accompanied by high sediment influx into the basin and as such, are laterally continuous, sand-rich and possess very good porosities, high net-to-gross values and negligible volumes of clay. They also possess appreciable amounts of hydrocarbon accumulation.

SOM facies analysis shows that within these reservoirs, the gross thicknesses include units of sandstone, shaly sandstone, shale and some coaly facies; especially towards the eastern part of the field. In the absence of core data this methodology, proves to be reliable in facies identification. Lastly, this study established that proper estimation of reservoir petrophysical properties and subsequent modelling of flow geology is dependent on a holistic understanding of facies type and distribution.

Acknowledgements

The authors wish to appreciate the Shell Petroleum Development Corporation (SPDC) for providing the dataset for this study and Petroleum Technology Development Fund (PTDF) for the support during the course of this research.

References

- [1] Abdel-Fattah MI. Impact of depositional environment on petrophysical reservoir characteristics in Obaiyed Field, Western Desert, Egypt. *Arab. J. Geosci.*, 2015; 8(11): 9301-9314.
- [2] Mira A, El-Behairy A, El-Rahman MMA, Naby MA, & Rizk M. Generic Approach of Integrating Core Data, and Petrophysical Interpretation to Generate Reliable Facies Model in Absence of Seismic Attribute Analysis-West Qarun Field Case Study. In SPE North Africa Technical Conference and Exhibition. OnePetro. (2015, September).
- [3] El-Gendy NH, Radwan AE, Waziry MA, Dodd TJ, & Barakat, MK. An integrated sedimentological, rock typing, image logs, and artificial neural networks analysis for reservoir quality assessment of the heterogenous fluvial-deltaic Messinian Abu Madi reservoirs, Salma field, onshore East Nile Delta, Egypt. *Mar. Petrol. Geol.*, 2022; 145, 105910.
- [4] Mode AW, Anyiam OA, & Omuije JO. Analysis of sedimentary facies and paleo-depositional environments of the DC70X reservoir in Mbakan field of the central swamp Niger Delta. *Arab. J. Geosci.*, 2015; 8: 7435-7443. <https://doi.org/10.1007/s12517-014-1690-6>.
- [5] Dim CIP, Onuoha KM, Mode AW, Okwara IC, & Okeugo CG. Characterizing the middle-upper Miocene reservoir intervals of a producing field in the Niger Delta Basin: an application of facies, sequence stratigraphic and petrophysical analyses. *Arab. J. Sci. Eng.*, 2019; 44(1): 429-448.
- [6] Eradiri JN, Odafen EE, Okwara IC, Mode AW, Anyiam OA, Ulasi NA, & Umeadi MI. Sedimentary facies and petrographic analyses of Miocene nearshore deposits, Central Swamp Depobelt, onshore Niger Delta Basin: Implications of reservoir quality. *J. Sed. Env.*, 2021; 6(4): 665-680.

- [7] Abdel-Fattah MI, Mahdi AQ, Theyab MA, Pigott JD, Abd-Allah ZM, & Radwan AE. Lithofacies classification and sequence stratigraphic description as a guide for the prediction and distribution of carbonate reservoir quality: a case study of the upper cretaceous Khasib formation (East Baghdad Oilfield, Central Iraq). *J. Pet. Sci. Eng.*, 2022; 109835.
- [8] Bressan TS, de Souza, MK, Girelli TJ, & Junior FC. Evaluation of machine learning methods for lithology classification using geophysical data. *Comput and Geosci*, 2020; 139, 104475.
- [9] Siddiqui NA, Rahman AH. A., Sum CW, Yusoff WI. W., & Ismail, M. Shallow-marine sandstone reservoirs, depositional environments, stratigraphic characteristics and facies model: a review. *J. Appl. Sci.*, 2017; 17(5): 212–237.
- [10] Anyiam OA, Eradiri JN, Mode AW, Okeugo CG, Okwara IC, & Ibemesi PO. Sequence stratigraphic analysis and reservoir quality assessment of an onshore field, Central Swamp Depobelt, Niger Delta Basin, Nigeria. *Arab. J. Geosci.*, 2019; 12(24): 1-19.
- [11] Odezulu C, Olawale S, Saikia K, & Mento D. Effect of Sequence Stratigraphy-based Facies Modelling for Better Reservoir Characterization: A Case Study from Powder River Basin. In Abu Dhabi International Petroleum Exhibition and Conference. *One Petro.* (2014, November)
- [12] Van Wagoner JC, Mitchum RM, Campion KM, & Rahmanian VD. (1990). Siliciclastic sequence stratigraphy in well logs, cores, and outcrops: concepts for high-resolution correlation of time and facies. *American Association of Petroleum Geologists, Volume 7*, ISBN electronic: 9781629810164. <https://doi.org/10.1306/Mth7510>.
- [13] Ogbe OB. Sequence stratigraphic controls on reservoir characterization and architectural analysis: a case study of Tovo field, coastal swamp depobelt, Niger Delta Basin, Nigeria. *Mar. Petrol. Geol.*, 2020; 121, 104579.
- [14] Elhossainy MM, Salman AM, Sarhan MA, Al-Areeq NM, & Alrefae HA. Sequence stratigraphic analysis and depositional evolution of the Upper Cretaceous deposits in Ras Budran oil field, Gulf of Suez, Egypt. *Arab. J. Geosci.*, 2021; 14(12): 1-13.
- [15] Abdel-Fattah MI, Sen S, Abuzied SM, Abiou, M, Radwan AE, & Benssaou M. Facies analysis and petrophysical investigation of the Late Miocene Abu Madi sandstones gas reservoirs from offshore Baltim East field (Nile Delta, Egypt). *Mar. Petrol. Geol.*, 2022; 137, 105501.
- [16] Al-Jawad SN, & Saleh AH. Flow units and rock type for reservoir characterization in carbonate reservoir: case study, south of Iraq. *J. Petrol Explor Prod Technol.*, 2020; 10(1): 1-20.
- [17] Al, A, Sheng-Chang C, & Shah M. Integration of Cluster Analysis and Rock Physics for the Identification of Potential Hydrocarbon Reservoir. *Nat. Resour. Res.*, 2021; 30(2): 1395–1409.
- [18] Puskarczyk E. Application of Multivariate Statistical Methods and Artificial Neural Network for Facies Analysis from Well Logs Data: An Example of Miocene Deposits. *Energies*, 2020; 13(7): 1548.
- [19] Okon AN, Adewole SE, & Uguma EM. Artificial neural network model for reservoir petrophysical properties: porosity, permeability and water saturation prediction. *Model. Earth Syst. Environ.*, 2021; 7(4): 2373-2390.
- [20] Dixit N, McColgan P, & Kusler K. Machine learning-based probabilistic lithofacies prediction from conventional well logs: A case from the Umiat Oil Field of Alaska. *Energies*, 2020; 13(18): 4862.
- [21] Hussain M, Liu S, Ashraf U, Ali M, Hussain W, Ali N, & Anees A. Application of Machine Learning for Lithofacies Prediction and Cluster Analysis Approach to Identify Rock Type. *Energies*, 2022; 15(12): 4501.
- [22] Saugy L, Eyer JA. Fifty years of exploration in the Niger delta (west Africa). In: Halbouty, M. T. (Ed.), *Giant Oil and Gas Fields of the Decade 1990 – 1999*, AAPG Mem., 2003; 78: 211–226.
- [23] Evamy BD, Haremboure J, Kamerling P, Knaap WA, Molloy FA, Rowlands PH. Hydrocarbon habitat of tertiary Niger delta. *AAPG Bull.*, 1978; 62: 1–39.
- [24] Stacher P. Present understanding of the Niger Delta hydrocarbon habitat; In: M. N. Oti and G. Postma (Eds.), *Geology of deltas*; A. A. Balkema, Rotterdam 1995; pp. 257–267.
- [25] Reijers TJA. Stratigraphy and sedimentology of the Niger Delta. *Geologos*, 2011; 17(3): 133-162.
- [26] Doust H, and Omatsol, E. Niger Delta: in Edwards, J. D., and Santogrossi, P. A., (Eds.), *Divergent/passive margin basins*: AAPG Mem., 1990; 48: 239-248.
- [27] Kulk, H. (1995). Regional petroleum geology of the world Part II: Africa, Africa, America Australia and Antarctica (pp. 143–172). Gebruder Borntraeger.
- [28] Haq BU, Hardenbol J, & Vail PR. (1988). Mesozoic and Cenozoic Chronostratigraphy and Cycles of Sea-level Change, In: C. K. Wilgus et al. (Eds), *Sea-Level changes: an integrated approach*: Society of Economic Paleontologists and Mineralogists, Special Publication 42, pp. 71-108.

- [29] Vail PR. Seismic stratigraphy interpretation, using sequence stratigraphy. Part I: Seismic stratigraphic procedure. [In:] A. W. Balley (Ed.): Atlas of seismic stratigraphy 1. Am Asso. Petrol. Geol. Studies in Geology, 1987; 27: 1-10.
- [30] Larionov VV. Borehole radiometry. U.S.S.R. Nedra, Moscow 1969.
- [31] Simandoux P. Dielectric measurements in porous media and application to shaly formations. Revue de Inst. Franc. Du Petrole, 1964; supplementary issue.
- [32] Kohonen T. Self-organizing maps: Third extended addition, Springer 2001, Series in Information Services.
- [33] Wu Y, & Takatsuka M. Spherical self-organizing map using efficient indexed geodesic data structure. Neural Netw., 2006; 19(6-7): 900-910.
- [34] Emery D, & Myers K. Sequence Stratigraphy. Blackwell 1996, London, 297 p.
- [35] Kendall C. Use of well logs for sequence stratigraphic interpretation of the subsurface. USC Sequence Stratigraphy., University of South Carolina 2003.
- [36] Shepherd M, Deltaic reservoirs, American Association of Petroleum Geologists Memoir 91. in M. Shepherd (ed), Oil Field Production Geology, 2009; 279-288.
- [37] Selley RC. Elements of petroleum geology. Academic Press 1998, San Diego, p 470.
- [38] Rider, M. H. (1986) The geological interpretation of well logs. Blackie, Glasgow, pp 151-165.
- [39] Osinowo OO, Ayorinde JO, Nwankwo CP, Ekeng OM, & Taiwo OB. Reservoir description and characterization of Eni field Offshore Niger Delta, southern Nigeria. J. Petrol. Explor. Prod. Technol., 2018; 8(2): 381-397.
- [40] Akaerue EI, Nnakuba JN, Urang JG, Ebong ED, Eradiri JN, & Ubgaja AN. Electro-sequence analysis and natural resources potential of a transitional environment in central swamp Depobelt, Niger Delta, Nigeria. J. Petrol. Explor. Prod. Technol, 2022; 12: 2381-2403.
- [41] Illo CA, Ugbor CC, Eradiri JN, & Emedo CO. Prospect identification and reservoir characterization using seismic and petrophysical data in 'Famito' field, onshore Niger Delta, Nigeria. Arab. J. Geosci., 2022; 15(4): 1-16.
- [42] Weber KJ. Sedimentological aspects of oil fields in Niger Delta. Geol.en Mijn., 1977;50: 559-576.
- [43] Anyiam O, Mode A, Okpala C B, & Okeugo C. The Use of Lorenz Coefficient in the Reservoir Heterogeneity Study of a Field in the Coastal Swamp, Niger Delta, Nigeria. Pet. and Coal, 2018; 60: 560-569 .

*To whom correspondence should be addressed: Joseph Nanaoweikule Eradiri, Petroleum Technology Development Fund, Department of Geology, University of Nigeria, Nsukka, Nigeria; e-mail: josepheradiri@gmail.com
<https://orcid.org/0000-0001-6141-052X>*